A. Murgai W. J. Patrick J. Combronde J. C. Felix

# Oxygen Incorporation and Precipitation in Czochralski-Grown Silicon

Oxygen incorporation is examined for growth of large-diameter (80–130 mm) silicon single crystals by the Czochralski method. The primary growth parameters affecting the oxygen concentration in the crystals are shown to be the crystal-melt interface position within the hot zone and the rate of crucible rotation used. Tight control of the oxygen concentration  $[\pm 1.5]$  parts per million atomic (ppma) in the range of 25–40 ppma (ASTM)] has been reproducibly attained by programmed variation of these growth parameters. The attainable oxygen concentrations may be extended over a wider range (20–45 ppma) through slight modifications of the hot zones. Wafers from the uniform-oxygen-concentration crystals are subjected to single-step and two-step annealing procedures (700–1100°C) for oxygen precipitation studies. The rate of precipitation is shown to depend on the initial oxygen content and on the number of initially unpopulated nucleation sites present.

#### Introduction

Significant amounts of oxygen (above the solid silicon solubility limit) are introduced in Czochralski silicon [1-4] from the silica liner in which the melt is contained. The distribution of this oxygen in the crystal is influenced by the growth parameters used [2, 3, 5-10]. During the high-temperature heat treatments normally used in the processing of integrated circuits, the oxygen forms SiO, micro-precipitates [6, 11-15] that can getter metallic impurities. These precipitates have been used effectively for "internal gettering" [16] during the fabrication of large-scale integrated (LSI) devices. Normally, it is desirable to have a uniform distribution of the internal gettering sites, and hence, a uniform oxygen distribution in the silicon. For metal-oxide-silicon (MOS) applications, we have found that high oxygen concentrations [O] can often result in high device yields. On the other hand, lower oxygen concentrations are found to be favorable for fabrication of bipolar devices.

This article examines the primary growth parameters affecting [O] during large-diameter (80-130 mm) growth of the Czochralski silicon. Programmed variations in these

parameters are used to attain crystals with uniform oxygen concentrations. Subsequent precipitation of oxygen, caused by high-temperature annealing of the wafers made from these crystals, is also examined. The precipitation is eliminated in a small zone (precipitate-free zone, PFZ) near the wafer surface. Parameters affecting the PFZ are discussed.

# **Experimental procedure**

Dislocation-free (100) silicon crystals with diameters up to 130 mm were grown by the Czochralski method from melt charges (up to 20 kg) contained in silica crucibles. During the crystal growth, counter-rotations [1-35 revolutions per minute (rpm)] of the crystal and crucible were used. In certain experiments, the crucible rotation rate was varied continuously through the above range. The crucible was also raised within the hot zone from specific starting locations at rates that were at all times a constant fraction of the instantaneous pull rate. The rates were generally one to two times the average rate at which the melt surface was lowered into the crucible during growth, referred to as the melt replacement rate (MRR). All silicon crystal boules in the

© Copyright 1982 by International Business Machines Corporation. Copying in printed form for private use is permitted without payment of royalty provided that (1) each reproduction is done without alteration and (2) the *Journal* reference and IBM copyright notice are included on the first page. The title and abstract, but no other portions, of this paper may be copied or distributed royalty free without further permission by computer-based and other information-service systems. Permission to *republish* any other portion of this paper must be obtained from the Editor.

above studies were pulled with a flat-top geometry at rates of 60-115 mm/h, with corrections to the pull rate of  $\pm 15\%$  being applied for automatic control of the crystal diameter. Growth was conducted in an argon atmosphere either under partial vacuum or at atmospheric pressure, with flow rates of 40-120 liters/min. The crystals were grown from two different types of pullers: one (A) had a dc graphite heater; the other (B) used a three-phase ac heater [8].

Oxygen incorporation/precipitation studies were conducted from measurements made on cross-sectional slices either ≈1.5 mm or 0.4 mm thick, taken at periodic intervals along the crystal length. The slices were chemically etched and chemomechanically polished to a mirror finish on both surfaces for the measurements. Oxygen concentrations were determined using the observed absorption at 1106 cm<sup>-1</sup> (ASTM-F121-76), which was measured with a dispersive or Fourier-transform infrared spectrophotometer. The densities of precipitate particles were either measured directly with the bevel-and-etch method [17] or computed from oxygen-precipitation kinetics [18].

# Models of oxygen incorporation

The variation in oxygen concentration along the longitudinal crystal axis during crystal growth may be obtained from a nonsteady-state consideration of the net flux rate, dQ/dt (g/s), of oxygen introduced into the melt from dissolution [19] of the silica crucible [at a rate W (g/cm²-s)] less the rates at which oxygen evaporates at the melt-ambient interface and at which it is incorporated into the growing crystal:

$$dQ/dt = W(L)A_1(L) - E^*q(L)A_2 - K_eq(L)VA_3, \qquad (1)$$

where  $A_1(L)$ ,  $A_2$ , and  $A_3$  are the areas of the crucible-melt, melt-ambient, and crystal-melt interfaces (cm²), L is the fraction of the melt which was solidified,  $E^*$  is the evaporation coefficient for SiO (cm/s), q(L) is the concentration of oxygen in the melt ( $g/\text{cm}^3$ ),  $K_c$  is the effective segregation coefficient of oxygen [4], and V is the crystal growth rate (cm/s) [20]. The detailed solutions to Eq. (1) have been given elsewhere [21] for both variable and constant dissolution rates, W(L) and  $W_0$ , respectively. During the time interval following the melting of solid silicon but prior to the start of crystal growth, a steady state of the net rate of oxygen flux into the melt is established [9]. However, in order to obtain a uniform axial oxygen distribution in the crystal,  $C_{s_u}$  (atoms/cm³), it is readily seen that the following condition must be satisfied during growth:

$$C_{s_u} = \left[ \frac{K_e W A_1}{E^* A_2 + V A_3 (K_e - 1)} \right] \left( \frac{2N_a}{A_1} \right) = \text{constant},$$
 (2)

where  $N_a$  is Avogadro's number and  $A_t$  is the atomic weight of SiO<sub>2</sub>. Under constant pressure and Ar flow rates, Eq. (2) implies that  $W(L) = \text{constant}/A_1(L)$ . That is, as the area of the crucible-melt interface is decreased during growth, the

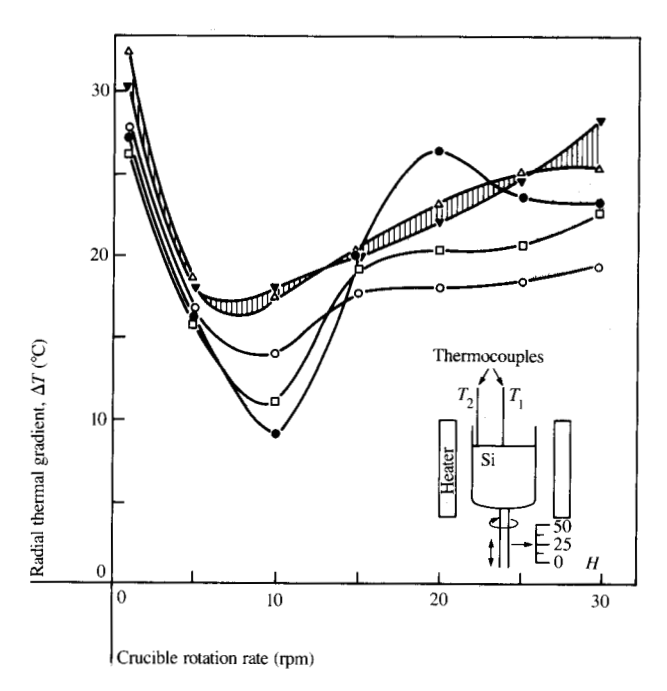


Figure 1 Variation in radial thermal gradient  $\Delta T (= T_2 - T_1)$  with the rate of crucible rotation for different crucible positions H in the hot zone (three-phase ac heater); crucible diameter = 203 mm, 9-kg melt. The various crucible positions (in mm) are designated by  $\bullet$  (0),  $\Box$  (13),  $\circ$  (25),  $\Delta$  (38), and  $\mathbf{v}$  (50). The shaded region represents the working level for crystal pulling.

**Table 1** Oxygen concentration vs, the crucible position in the hot zone.

Rotation rates of crystal, crucible (rpm)	Crucible position (mm)	Thermocouple output (pu) <sup>a</sup>	C <sub>so</sub> (ppma)	Crucible type <sup>b</sup>
8, -8	0	1360	31.6	С
	-38	1246	24.4	O
	-38	1250	24.5	O
	-38	1255	25.2	O
30, -10	0	1376	33.8	C
	-13	1353	32.4	C
	-13	1347	31.8	C
	-25	1302	31.8	C
	-25	1260	30.3	O
	-38	1242	28.4	O

<sup>a</sup>Proportional units

<sup>b</sup>C = "clear" and O = "opaque," as classified by vendors

dissolution rate of the silica crucible must be increased by changing other growth parameters in order to attain a uniform axial oxygen concentration in the crystal.

# Results and discussion

#### Oxygen incorporation

The effects of various growth parameters on seed-end oxygen concentration  $C_{s_0}$  [22] have been shown elsewhere [9] to

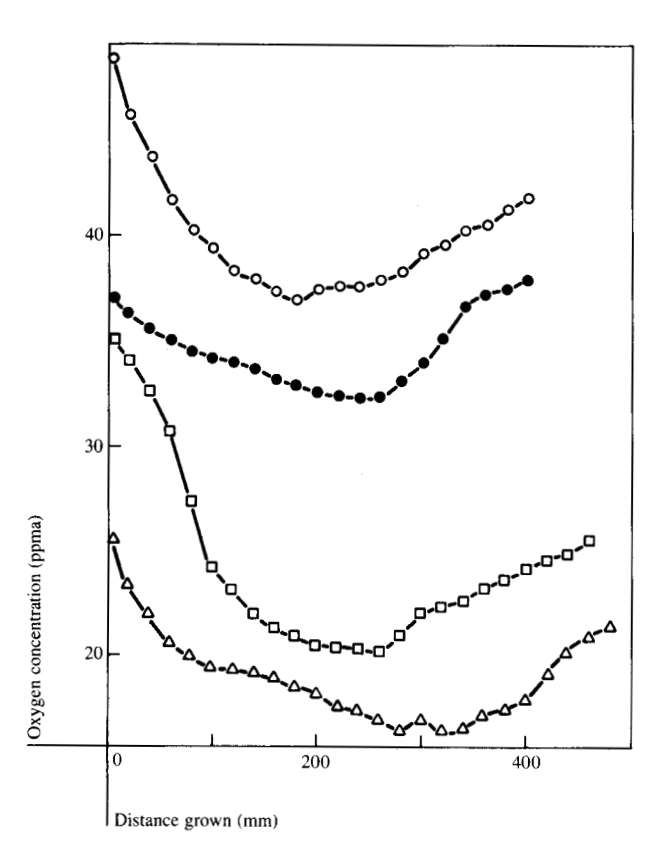


Figure 2 Variation in  $C_{so}$  and axial profile with rate of crucible rotation:  $8 \text{ rpm } (\Delta)$ ,  $15 \text{ rpm } (\Box \text{ and } \bullet)$ , and  $25 \text{ rpm } (\circ)$  (three-phase ac heater). Crystal diameter = 83 mm, crucible diameter = 203 mm, pull rate = 75 mm/h, crystal rotation rate = 22 rpm, 9-kg melt. In the high-level process (o and  $\bullet$ ), crucible rotation was stopped periodically for short durations during growth, which resulted in a higher oxygen concentration than that produced by the medium-level process ( $\Box$  and  $\Delta$ ).

**Table 2** Tail-end oxygen concentration  $\nu s$ . crucible lift rate. Crystal pull rate of 100 mm/h, crystal rotation rate of 8 rpm, crucible rotation rate of -8 rpm, crystal diameter of 82.5 mm, and 12-kg silicon charge.

$\frac{C_{\rm L}}{({ m mm/h})}$	Tail-end [O] (ppma)
12	24
13	26
14	27
15	28
16	29

conform with the steady-state relation,

$$C_{s_0} = \left[ \frac{K_e W A_1}{E^* A_2} \right]_{L=0} \left( \frac{2N_a}{A_1} \right). \tag{3}$$

The variations in concentration (hence,  $E^*$ ) with partial

vacuum gas pressure (2-7 kPa) were shown to be negligible. However, the maximum variation in concentration (and W) is found with variations both in the starting crucible height in the hot zone and in the crucible rotation rates (Fig. 1). The effect of the crucible height is shown in Table 1 for crystals pulled with crystal rotation rates of either 30 or 8 rpm. A direct correspondence can be seen between the output of the heater control thermocouple and  $C_{so}$ . The variations in the heater control thermocouple output indicate corresponding variations in radial thermal gradients (average crucible wall temperatures, hence, W), since crystal growth is always established with the crystal-melt interface at the melting point (a constant). This then results in the observed variations in oxygen concentration when the crucible height is varied. With this method  $C_{s_0}$  was reproducibly varied over the range of 25-40 parts per million atomic (ppma) (resulting from variations in crucible dissolution rates by nearly a factor of 1.8). In addition to being a function of the crucible height, small variations in the oxygen concentration were found, depending on either the crucible type ("opaque" or "clear," as classified by the vendors) or the crystal rotation rate (8 or 30 rpm). However, the range of variation caused by these parameters was significantly smaller than that attainable by varying the crucible height.

In puller B, the variation in radial thermal gradients under varying crucible rotation rates was determined directly from two silica-sheathed thermocouples immersed at the center and periphery of 9-kg melts (Fig. 1). The variation in [O] for crystals pulled under different crucible rotation rates (kept constant during growth in these experiments) is shown in Fig. 2. The increase in [O] with increasing crucible rotation rates [23] is consistent with the increase in radial thermal gradients, as seen in Fig. 1. Furthermore, the initial decrease in axial oxygen concentration seen in Fig. 2 was found to be typical of crystals pulled under growth conditions normally used. (The subsequent increase in oxygen concentration at the tail-end of crystals in Fig. 2 may be related to a significant increase in the radial thermal gradients for the hot zone of puller B during the last portions of melt solidification. A further treatment of this phenomenon is given for puller A in the following discussion.) The detailed aspects of axial variations in [O] have been discussed elsewhere [21]; it was shown semiquantitatively that the axial decrease in oxygen is related to decreasing  $A_1(L)$  during growth. [See also Eq. (2).] Thus, axial uniformity in oxygen may be attained by a programmed increase in the crucible rotation rate to compensate for the above decrease in  $A_1(L)$  during growth. In conjunction, crucible lift rates  $C_r$  that are higher than MRR may also be used during growth. The effect of  $C_L > MRR$  is shown in Table 2 for crystals pulled at 100 mm/h from 12-kg melts in puller A. Use of a  $C_L > MRR$ results in progressively higher positions of the crystal-melt interface in the hot zone and, as seen in Table 1, in increasing

548

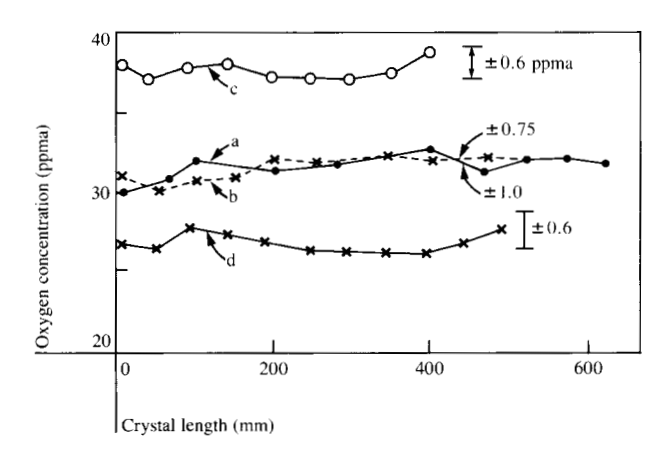


Figure 3 Uniformity in axial oxygen concentrations obtained through programmed variation of crucible rotation rates;  $C_L >$ MRR. Plot a: Puller A; crystal diameter = 100 mm, pull rate = 51 mm/h, rotation rate = 28 rpm, crucible diameter = 305 mm, lift rate = 10 mm/h, counter-rotation rate =  $9 \pm 2.5$  rpm/(0.1L) (average), 18-kg melt. Plot b: Puller A; crystal diameter = 125 mm, pull rate = 57 mm/h, lift rate = 17 mm/h, and counter-rotation rate =  $10 \pm 2.5 \text{ rpm/}(0.1L)$  (average); all other parameters as in Plot a. For Plots c and d: Puller B; crystal diameter = 83 mm, pull rate = 75 mm/h, rotation rate = 22 rpm, crucible diameter = 254 mm, lift rate = 16 mm/h, and counter-rotation rates =  $13 \pm 1.3$ rpm/0.1L (average) and  $14 \pm 2.5 rpm/0.1L$  (average), respectively, for 9-kg melts. In Plot c the crucible rotation was stopped at periodic intervals for short durations during growth (same as for the highlevel process in Fig. 2). This resulted in a higher oxygen level than in Plot d.

radial thermal gradients during growth. As Table 2 shows,  $C_{s_0}$  is consistently higher for the higher crucible lift rates.

From Eq. (2), it is readily seen that the total increments required in the crucible rotation and lift rates and the conditions for attaining axial uniformity in the oxygen concentration depend on the nominal pull rate used. Accordingly, the fractional variation in oxygen concentration,  $\Delta C_{s_a}/C_{s_a}$ , with variation in pull rate  $\Delta V$  is obtained from the derivative of Eq. (2) and from Eq. (3):

$$\frac{\Delta C_{s_u}}{C_{s_u}} \approx -\frac{\Delta V A_3}{E^* A_2} (K_e - 1). \tag{4}$$

The variations in pull rate and heater power are normally used in a closed loop for automatic diameter control. Thus, in our apparatus, for growth of 100-mm-diameter crystals having a uniform 35-ppma oxygen concentration, it was found that a 13 mm/h average variation in the pull rate resulted in a 2-ppma variation in the oxygen concentration.

Figure 3 shows typical axial profiles of uniform-oxygenconcentration crystals grown in pullers A and B from 18- and 9-kg melts, respectively. In puller A, both ramping of the crucible rotation rate (rates varied continuously during growth) and crucible lift rates in excess of MRR were used;

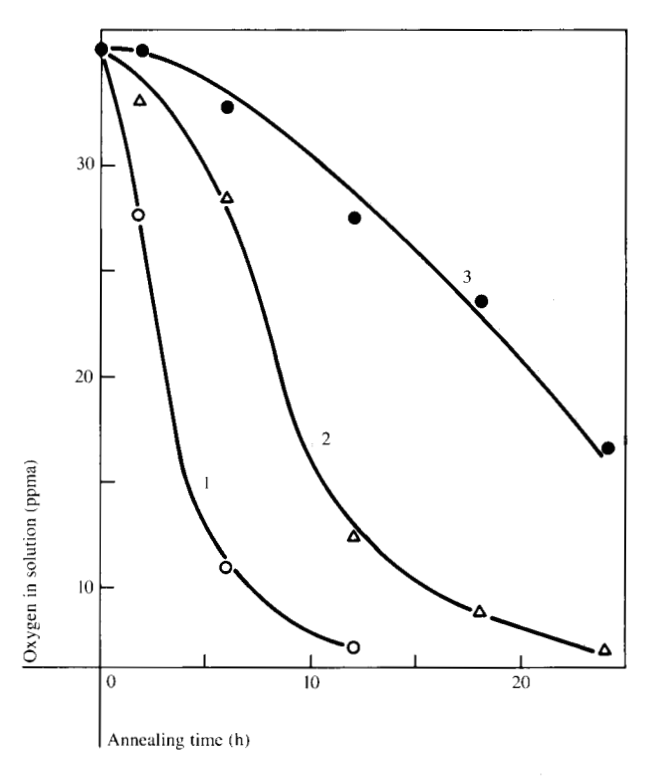


Figure 4 Oxygen in solution as a function of annealing time. The respective annealing temperatures T (in °C), time constants for precipitation  $\tau$  (in h<sup>-2</sup>), and number of precipitate particles  $N_p$  for each plot are as follows. Plot 1: 800, 6.8, 6.0 × 10<sup>12</sup>; Plot 2: 750, 13.0, 1.5 × 10<sup>13</sup>; and Plot 3: 700, 31.5, 3.2 × 10<sup>13</sup>. When the log of the fraction of the oxygen remaining in solution is plotted, a portion of the curve is exponential and its slope  $\tau$  allows calculation of  $N_p$ .

in puller B, only ramping of the crucible rotation was used during growth. The detailed growth parameters are indicated in Fig. 3. As can be seen, a high degree of axial uniformity was attained with these methods.

Since evaporation of the SiO has been shown [21] to be diffusion-limited by a boundary layer at the melt-ambient interface, radial uniformity in the oxygen concentration [O] is controlled primarily by the prevailing hydrodynamics of the melt. For the uniform-oxygen-concentration crystals just discussed, radial uniformity was attained by using a fast crystal-rotation rate throughout the growth period.

### • Oxygen precipitation

The precipitation of oxygen in silicon can be followed by observing the decrease in the intensity of the absorption caused by heat treatments at different temperatures. Figure 4 shows results obtained on three separate quarter sections of a single wafer, which were annealed at different temperatures. Patrick has demonstrated that the precipitation kinetics can be described as diffusion-limited [24]. Thus, we may

549

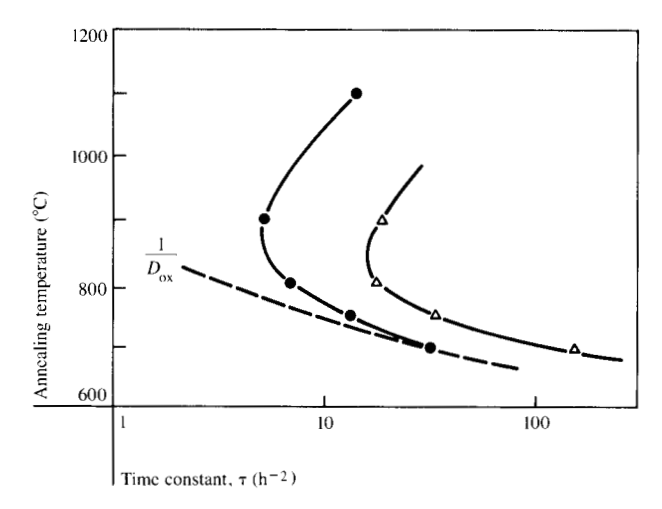


Figure 5 The time constant for precipitation  $\tau$  vs. the annealing temperature T for two oxygen concentrations: 28 ( $\Delta$ ) and 35 ( $\bullet$ ) ppma. The dotted curve marked  $1/D_{ox}$  is the reciprocal of the oxygen diffusion coefficient plotted to this same scale and translated along the  $\tau$  axis to match the low-temperature arm of the 35-ppma curve ( $\bullet$ — $\bullet$ ).

**Table 3** Number of precipitate particles vs. the pre-annealing conditions and the initial oxygen concentration.

Initial [O] (ppma)	Pre-annealing conditions <sup>a</sup> (10 <sup>8</sup> cm <sup>-3</sup> )	$N_{\mathtt{p}}$
33	A	0.64
	В	0.89
	C	97
	none	_
26	Α	1.0
	В	1.4
	C	53
	none	1.3

 $<sup>^{</sup>a}A = 1200$  °C for 1 h; B = 1200 °C for 1 h followed by 820 °C for 5 h; C = 820 °C for 5 h.

compute the number of precipitate particles  $N_p$  [25] from the observed rate. Two wafers from the same section of crystal, having identical oxygen concentrations, were quartered. Five of the quarters were annealed sequentially (as in Fig. 4) at temperatures increasing from 700 to  $1100^{\circ}$ C. The same annealing steps were repeated for another quartered wafer with a lower oxygen concentration; Fig. 5 shows the results. The value of  $\tau$ , the time constant for the precipitation obtained from the sequential annealing, is plotted as a function of annealing temperature. A C-shaped curve is observed, similar to the curves seen in temperature-time-transformation (TTT) plots. The maximum rate depends on the initial oxygen content and the number of particles growing. The rate decreases at low temperature because of the decrease in diffusivity of the oxygen  $(D_{\infty})$ . In fact, if one

plots the reciprocal of  $D_{\rm ox}$  on this same scale, the slope of the low-temperature arm of the TTT curve approaches a curve parallel to  $1/D_{\rm ox}$  (dashed curve in Fig. 5). This indicates that the precipitation rate and the activation energy for the diffusion are the same. Computed values of  $N_{\rm p}$  are plotted in Fig. 6;  $N_{\rm p}$  is a monotonically decreasing function of temperature. The decrease in the precipitation rate on the high-temperature arm of the TTT curve results from the smaller number of particles being nucleated at the higher temperatures.

These results can be modified by using a two-step annealing process, wherein nucleation of the precipitates is accomplished at the first temperature and precipitation is carried out at a second temperature. Two wafers were quartered and each quarter was subjected to a separate pre-annealing step. The precipitation kinetics were then followed at 1050°C. The results are shown in Table 3.

In the samples which saw no separate pre-annealing,  $N_{\rm p}$  depended on both the thermal history of sections during crystal pulling and the initial oxygen concentration. Quarters which received the high-temperature pre-anneal had few precipitates, while those receiving the low-temperature pre-anneal had considerably higher numbers of precipitate particles. Consistently, the high-low combination produced few precipitates. This indicated 1) that the high-temperature treatment was responsible for the destruction of embryonic precipitates present in the as-grown material and 2) that the low-temperature-annealed sample (annealing condition C in Table 3) did not nucleate appreciably large numbers of new particles.

Another consideration in the precipitation of oxygen is the formation of a region free of precipitates near the surface of the sample [26]. Oxygen atoms near the surface can diffuse either to precipitate particles or to the sample surface during the high-temperature anneal. If precipitation occurs very rapidly, a precipitate-free zone (PFZ) is not formed, and the SiO<sub>2</sub> particles extend almost to the surface. Table 4 shows the results of an experiment where samples were first preannealed at 800°C for various times and then annealed for 24 h at 1050°C to precipitate the oxygen.

In the experiment, four wafers were quartered and each quarter received the indicated low-temperature pre-anneal. In all instances, this initial treatment led to a reduction in the width of the PFZ. The results demonstrate that this type of pre-anneal leads to rapid precipitation because it increases the number of  $\mathrm{SiO}_2$  particles. Thus, in a sense, the width of the PFZ is a function of  $N_\mathrm{p}$ , which in turn depends on the oxygen content, any prior thermal history, and the existing embryo population. The width of the PFZ thus depends on the oxygen precipitation rate.

#### Summary and conclusions

Radial thermal gradients (crucible wall temperatures) were shown to be critically determined by both the crucible position in the hot zone and the rate of crucible rotation during growth of Czochralski silicon crystals. Thus, through these parameters, one can vary both the silica crucible dissolution rates (by a factor nearly as large as two) and the oxygen concentration (from 25–40 ppma). Crystals with uniform oxygen concentrations were obtained by the programmed variation of these parameters during growth for crystals up to 125 mm in diameter pulled from 9- and 18-kg melts. This method could be extended, in general, to other sizes of crystals and melts.

Oxygen-precipitation rates were shown to depend on the initial oxygen content, on the existing embryo population, and on whether or not these sites are populated during appropriate thermal cycles. Thus, controlling the oxygen level may lead to control of the precipitation rates. This, in turn, can have practical benefits in the processing of integrated circuits.

#### References and notes

- S. E. Bradshaw, "The Contamination of Silicon by the Crucible," Solid State Physics in Electronics and Telecommunication, M. Desirant and J. L. Michels, Eds., Academic Press, Inc., New York, 1960; Vol. 1, Part 1, pp. 44-60.
- 2. W. Kaiser and P. H. Keck, "Oxygen Content of Silicon Single Crystals," J. Appl. Phys. 28, 882-887 (1957).
- A. J. Goss and R. E. Adlington, "The Effects of Seed Rotation on Silicon Crystals," *Marconi Rev.* 22, 28-43 (1959).
- Y. Yatsurugi, N. Akiyama, Y. Endo, and T. Nozaki, "Concentration Solubility and Equilibrium Distribution Coefficient of Nitrogen and Oxygen in Semiconductor Silicon," J. Electrochem. Soc. 120, 975-979 (1973).
- A. Murgai, H. C. Gatos, and W. A. Westdorp, "Effect of Microscopic Growth Rate on Oxygen Microsegregation and Swirl Defect Distribution in Czochralski-Grown Silicon," J. Electrochem. Soc. 126, 2240-2245 (1979).
- A. Murgai, J. Y. Chi, and H. C. Gatos, "Microdistribution of Oxygen in Silicon," J. Electrochem. Soc. 127, 1182-1186 (1980).
- T. Abe, K. Kikuchi, and S. Shirai, "Oxygen Striations in Silicon Crystals," Semiconductor Silicon—1977, H. Huff and E. Sirtl, Eds., Electrochemical Society, Princeton, NJ, 1977, pp. 95– 104.
- 8. K. Hoshikawa, H. Koda, H. Hirata, and H. Nakanishi, "Low Oxygen Content Czochralski Silicon Crystal Growth," *Jpn. J. Appl. Phys.* 19, 33-36 (1980).
- A. Murgai, "Parameters Affecting Oxygen Incorporation at the Seed-End of Czochralski-Grown Silicon Crystals," *Electro*chem. Soc. Ext. Abstr. 80-2, 1333-1335 (1980).
- B. M. Turovskii, "Distribution of Oxygen in Single Crystals of Silicon Growth by the Extracentral Czochralski Method," Izvestiya Akademii Nauk SSR, Neorganicheskie Materialy 11, 589-592 (1975).
- C. W. Pearce and G. A. Rozgonyi, "Source of Oxidation Induced Stacking Faults in Czochralski Silicon Wafers—II," Op. cit., Ref. 7, pp. 606-616.
- 12. J. T. Yue and H. T. Ruiz, "Precipitation in Czochralski Silicon Wafers During High Temperature Oxidation," *Op. cit.*, Ref. 7, pp. 596-605.

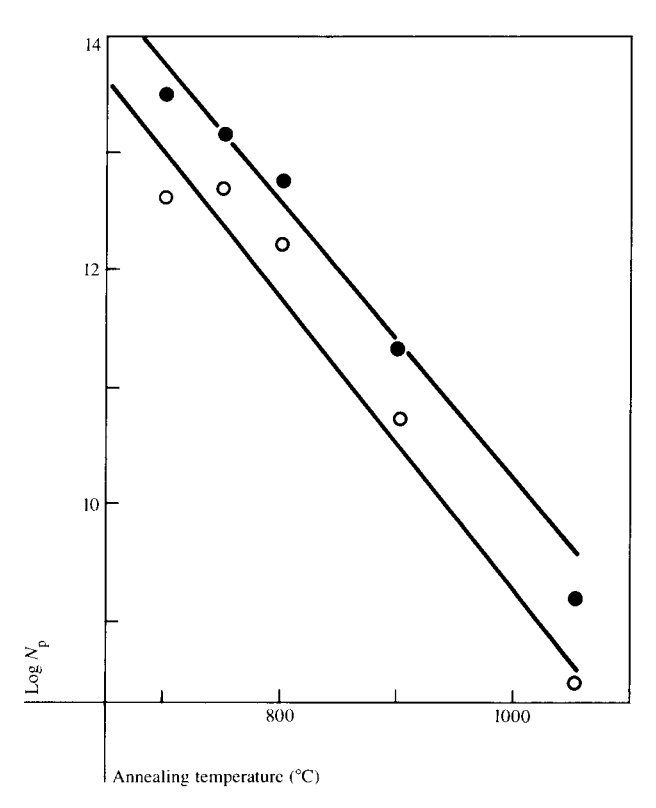


**Figure 6** Log  $N_p$  vs. annealing temperature T for values of  $N_p$  calculated from oxygen precipitation kinetics; [O] = 28 (o) or 35 ( $\bullet$ ) ppma.

Table 4 Width of the precipitate-free zone (PFZ) vs. the preannealing time (at 800°C) for varying oxygen concentrations.

Initial [O] (ppma)	PFZ widths (μm) for pre-annealing times (h):				
	24	6	2	0	
27	0	2	8	10	
28	0	9	10	15	
30	0	14	10	16	
38	0	0	3	8	

- 13. T. Y. Tan, E. E. Gardner, and W. K. Tice, "Intrinsic Gettering by Oxide Precipitate Induced Dislocations in Czochralski Silicon," Appl. Phys. Lett. 30, 175-176 (1977).
- M. Watanabe, M. Nakamura, and K. Homma, "Gettering of Defects in the Epitaxial Layer by Controlling Microdefects in the Substrate," *Electrochem. Soc. Ext. Abstr.* 79-2, 1244-1247 (1979).
- S. C. Baber, H. R. Huff, J. T. Robinson, H. Schaake, and D. Wong, "Some Observations of Bulk Oxygen Precipitation/ Gettering in Device Processed Czochralski Silicon," *Electrochem. Soc. Ext. Abstr.* 79-2, 1262-1266 (1979).
- 16. During heat treatment of silicon used in device fabrication, preferential diffusion of metallic impurities occurs towards the SiO<sub>2</sub> precipitate sites. These sites are designed to be situated away from the active regions of devices.

- 17. M. Wright-Jenkins, "A New Preferential Etch for Defects in Silicon Crystals," J. Electrochem. Soc. 124, 757-762 (1977).
- W. Patrick, E. Hearn, W. Westdorp, and A. Bohg, "Oxygen Precipitation in Silicon," J. Appl. Phys. 50, 7156-7164 (1979).
- 19. For large melts, the fractional oxygen contribution from dissolution at the crucible melt-ambient interface is negligibly small.
- 20. With the argon gas flowing under a partial vacuum and from top to bottom in puller A, carbon-free crystals (<0.1 ppma C) were grown reproducibly. A negligible increase in the oxygen in the melt is expected from any CO coming from the graphite heater. Also, for puller B operated at an atmospheric pressure of argon, this contribution is estimated to be less than 5% of the oxygen content.</p>
- 21. A. Murgai, "Mechanisms of Oxygen Incorporation in Czochralski Grown Silicon," *Op. cit.*, Ref. 7, pp. 113-125.
- 22. In this study  $C_{s_0}$  was determined from the average of concentrations at the center of three consecutive cross-sectional slices. The slices were taken near the top of the boule where the width of four (100) growth facets first becomes a minimum.
- 23. It may be noted that increased crucible rotation rates also result in increased melt mixing, which, in turn, will also contribute to the observed increase in [O].
- W. J. Patrick, "The Precipitation of Oxygen in Silicon and Its Effect on Surface Perfection," Silicon Device Processing, NBS Special Publication 337, National Bureau of Standards, Washington, DC, 1970, pp. 442-449.
- F. S. Ham, "The Theory of Diffusion-Limited Precipitation," J. Phys. Chem. Solids 6, 335-351 (1958). See Ref. 22 for experimental verification of this fact.
- W. J. Patrick, S. M. Hu, and W. A. Westdorp, "The Effect of SiO<sub>2</sub> Precipitation in Silicon On Generation Currents in MOS Capacitors," J. Appl. Phys. 50, 1399-1403 (1974).

Received September 1, 1981; revised April 21, 1982

Jacques Combronde

1BM France, Boîte Postale 58, 91102
Corbeil-Essonnes Cedex, France. Dr. Combronde joined IBM in 1973 with a Ph.D. in physics from the Institut National des Sciences Appliquées de Lyon, France. He is working as a pilot line engineer at the European Materials Competence Center.

Jean Claude Felix IBM France, Boîte Postale 58, 91102 Corbeil-Essonnes Cedex, France. Mr. Felix joined IBM in 1970 with a Brevet de Technicien Supérieur. He provided software support in the crystal growth development area until recently, when he assumed the position of manager in the post-processing mask data

IBM General Technology Division, East Ashok Murgai Fishkill facility, Hopewell Junction, New York 12533. Dr. Murgai joined IBM as a staff engineer in crystal growth development in East Fishkill in 1979. He helped develop the understanding of oxygen incorporation in large-diameter Czochralski silicon, the associated melt thermo-hydrodynamics, growth-related microdefects, and a number of processes for attaining uniform oxygen concentration crystals. In 1980 he became advisory engineer and in 1981 moved to advanced materials development. His present interests include preparation and characterization of bulk silicon for VLSI applications. He received his Sc.D. in materials science from the Massachusetts Institute of Technology in 1975. From 1975 to 1979, he worked on postdoctoral assignments successively at IBM and at the Massachusetts Institute of Technology. Dr. Murgai is a member of the Electrochemical Society.

William J. Patrick

IBM General Technology Division, East Fishkill facility, Hopewell Junction, New York 12533. Mr. Patrick received a B.S. in physics in 1957 from Manhattan College and an M.S. in physics from Syracuse University, New York, in 1965. He has been with IBM since 1960, working primarily in silicon materials technology: silicon epitaxy, crystal growth, and wafer processing. Presently, Mr. Patrick is in a chemical vapor deposition area, investigating the properties of dielectric films.